Singularities in the fluctuation of on-off intermittency

Takehiko Horita
Department of Mathematical Engineering and Information Physics, The University of Tokyo, Tokyo 113-8656, Japan

Hiromichi Suetani
NTT Communication Science Laboratories, NTT Corporation, 2-4 Hikaridai, Seika-cho, Soraku-gun, Kyoto 619-0237, Japan
(Received 6 December 2001; published 20 May 2002)

For a two-dimensional piecewise linear map exhibiting on-off intermittency, the scaling property of fluctuation, i.e., the large deviation property is investigated. It is shown that there are three phases of fluctuation and the q-weighted average of an observed quantity has singularities such as jumps or a plateau due to transitions between the phases. At the onset of on-off intermittency, the width of the plateau vanishes due to the disappearance of one of the three phases and the singularity becomes weaker but more probable. The singularity at the onset of on-off intermittency is also examined on the coupled logistic map.

DOI: 10.1103/PhysRevE.65.056217 PACS number(s): 05.45.−a

I. INTRODUCTION

On-off intermittency [1,2] and riddled basins [3] appear in nonlinear dynamical systems with invariant subspaces, where the dynamics restricted to the invariant subspace is chaotic. Due to the chaotic property of the dynamics in the invariant subspace, on-off intermittency and riddled basins possess considerable complexity despite its simple structure of the dynamics. In the present paper, we focus on on-off intermittency that has been investigated in many respects not only in low-dimensional dynamical systems [4–8] but also in continuously spatially extended systems [9].

For an understanding of complex behavior in nonlinear dynamical systems, the scaling property of fluctuation, which is formulated as thermodynamic formalism, is useful [10,11]. For example, the nonhyperbolicity of chaotic attractor due to homoclinic tangency is characterized by the discontinuity in the q-weighted average of local expansion rate [12]. The structure of riddled basin is characterized by a multifractal spectrum [13]. On-off intermittency is also characterized by its scaling property of fluctuation. The large deviation property, one of the scaling property of fluctuation, of on-off intermittency is investigated for the distance from the invariant subspace with a multiplicative noise model [5] and for the portion of time spent in the laminar phase with a piecewise linear map [8]. It is demonstrated that there appears a singularity in the q-weighted average of the observed quantity. The common feature of the above two models is the existence of underlying random walks, which is considered to be the origin of the observed singularity. This is suggested by the fact [14] that inhomogeneous random walks generate singularities in their thermodynamic structure functions. Our purpose in the present paper is to clearly demonstrate singularities in the fluctuation of on-off intermittency for piecewise linear maps by considering a set of observed variables.

In Sec. II, we introduce two piecewise linear maps that exhibit on-off intermittency. In Sec. III, we calculate the thermodynamic structure functions and show that there appear two types of singularities. A summary and concluding remarks concerning the nonhyperbolicity due to underlying random walks of on-off intermittency are given in Sec. IV.

II. PIECEWISE LINEAR MODELS OF ON-OFF INTERMITTENCY

We consider two-dimensional piecewise linear maps of the form

$$x_{n+1}=F(x_n), \quad y_{n+1}=G(x_n,y_n), \tag{1}$$

where $G(x,0)=0$ and thus $y=0$ is the invariant subspace. Assume that the restricted dynamics $x_{n+1}=F(x_n)$ to the invariant subspace is chaotic. If the transverse Lyapunov exponent

$$\lim_{N\to\infty}(1/N)\sum_{n=0}^{N-1}\ln|\partial G(x_n,0)/\partial y| \tag{2}$$

along an orbit on the invariant subspace converges and is less than zero, then the invariant subspace is transversally stable with respect to this orbit. If we have such an orbit with negative transverse Lyapunov exponent and the orbit is associated with the natural invariant measure of $x_{n+1}=F(x_n)$, then the invariant subspace contains an attractor in Milnor's sense [15]. On-off intermittency [1,2,6] is observed, if the following conditions are satisfied: (a) the invariant subspace contains no attractor, (b) there are orbits on the invariant subspace having negative transverse Lyapunov exponents, and (c) there is a global mechanism of reinjection. Note that the second condition enables the invariant subspace somewhat "attracting."

As a tractable model exhibiting on-off intermittency [7], we introduce the following simplified two-dimensional piecewise linear map:

$$x_{n+1}=F(x_n)=\begin{cases} x_n/a & \text{if } 0\leqslant x_n\leqslant a \\ (1-x_n)/(1-a) & \text{if } a<x_n\leqslant 1, \end{cases} \tag{3}$$

$$y_{n+1}=G(x_n,y_n)=\begin{cases} y_n/b & \text{if } 0\leqslant x_n\leqslant a, 0\leqslant y_n\leqslant b \\ by_n & \text{if } a<x_n\leqslant 1 \\ y_n & \text{if } 0\leqslant x_n\leqslant a, b<y_n\leqslant 1, \end{cases} \tag{4}$$

 ©2002 The American Physical Society

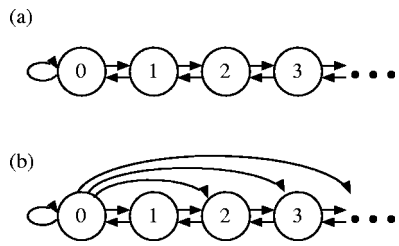

FIG. 1. Graphs of possible symbol sequence for the models (a) I and (b) II.

where $1/2<a<1$ and $0<b<1$ are constants. And we also consider another model [8] by replacing the dynamics in y with

$$y_{n+1}=G(x_n,y_n)=\begin{cases} y_n/b & \text{if } 0\leqslant x_n\leqslant a, 0\leqslant y_n\leqslant b \\ by_n & \text{if } a<x_n\leqslant 1, 0\leqslant y_n\leqslant b \\ (1-y_n)/(1-b) & \text{if } b<y_n\leqslant 1, \end{cases} \tag{5}$$

which is referred to as the model II while the first model is referred to as the model I in the following.

The natural invariant measure for the asymmetric triangular map $x_{n+1}=F(x_n)$ of Eq. (3) is the Lebesgue measure [16]. Since

$$\partial G(x,0)/\partial y=\begin{cases} b^{-1} & \text{if } 0\leqslant x\leqslant a \\ b & \text{if } a<x\leqslant 1, \end{cases} \tag{6}$$

if $a>1/2$, the condition (a) is satisfied and $a=a_0\equiv 1/2+0$ is the onset point of on-off intermittency. The condition (b) is also satisfied, since $x_{n+1}=F(x_n)$ has a set of initial conditions x_0 such that the orbit $\{x_n\}$ spends longer time in the interval $[0,a]$ than in the interval $[a,1]$. The condition (c) is satisfied as well. Let us consider a partition of the phase space $[0,1]\times[0,1]$ into rectangles

$$R_j\equiv[0,1]\times[b^{j+1},b^j], \quad j=0,1,2,\ldots. \tag{7}$$

With this phase space partition, a symbolic dynamics can be considered, where the graphs of possible symbol sequence have similar structures with random walks as shown in Fig. 1. More precisely, the rectangle $R_j\cap R^\alpha(\alpha=0,1, j=0,1,2,\ldots)$, where $R^0\equiv[0,a]\times[0,1]$ and $R^1\equiv[a,1]\times[0,1]$, is linearly mapped to

$$R_0 \quad \text{if } \alpha=j=0,$$

$$R_{j+2\alpha-1} \quad \text{otherwise}, \tag{8}$$

and

$$\cup_{k=0}^{\infty}R_k \quad \text{if } j=0,$$

$$R_{j+2\alpha-1} \quad \text{otherwise}, \tag{9}$$

in the models I and II, respectively.

III. LARGE DEVIATION PROPERTIES

In this section, we investigate large deviation properties [17] of on-off intermittency by introducing a set of observed variables and generalize the result shown in the previous paper [8], where only a certain variable is observed.

Let us consider a quantity $u(X)$ defined at each phase space point X. Its finite time average over n steps is

$$u_n(X)\equiv(1/n)\sum_{k=0}^{n-1}u(T^k(X)), \tag{10}$$

where T^k denotes kth iterate of the map T. Then the large deviation property [10,11] is characterized by

$$\langle\delta(u-u_n(X))\rangle\sim\exp[-nS(u)] \tag{11}$$

for large n with the fluctuation spectrum $S(u)$, where $\langle G(X)\rangle$ denotes the average with respect to the natural invariant measure. Note that $S(u)$ is a concave function taking its minimum value 0 at $u=\langle u(X)\rangle$. The thermodynamic structure functions associated with $u(X)$ are introduced by

$$\phi(q)\equiv\lim_{n\to\infty}(1/n)\ln\langle e^{nqu_n(X)}\rangle \tag{12}$$

and

$$u(q)\equiv d\phi(q)/dq=\lim_{n\to\infty}\langle u_n(X)e^{nqu_n(X)}\rangle/\langle e^{nqu_n(X)}\rangle, \tag{13}$$

where $-\infty<q<\infty$. The fluctuation spectrum $S(u)$ is related to $\phi(q)$ with the Legendre transformation

$$S(u)=\max_q\{qu-\phi(q)\}. \tag{14}$$

In the following, we consider

$$u(x,y)\equiv\begin{cases} u_0 & \text{if } 0\leqslant x<a, b<y\leqslant 1 \\ u_+ & \text{if } 0\leqslant x<a, 0\leqslant y\leqslant b \\ u_- & \text{if } a\leqslant x\leqslant 1, \end{cases} \tag{15}$$

for the model I and

$$u(x,y)\equiv\begin{cases} u_0 & \text{if } b<y\leqslant 1 \\ u_+ & \text{if } 0\leqslant x<a, 0\leqslant y\leqslant b \\ u_- & \text{if } a\leqslant x\leqslant 1, 0\leqslant y\leqslant b, \end{cases} \tag{16}$$

for the model II, where u_0, u_+, and u_- are constants. Note that a set of observed variables u can be considered by taking several values of u_0, u_+, and u_- and that the transverse expansion rate $u(x,y)=\ln|\partial G(x,y)/\partial y|$ can be considered with an appropriate choice of the values of u_0, u_+, and u_-.

Now we are interested in

$$M_q(n) \equiv \langle e^{nqu_n(X)} \rangle \tag{17}$$

$$= \int dX \rho(X) \exp\left[q \sum_{k=0}^{n-1} u(T^k(X)) \right] \tag{18}$$

$$= \int dX [\mathcal{H} e^{qu(x)}]^n \rho(X), \tag{19}$$

where $\rho(X)$ denotes the natural invariant density and $\mathcal{H}$ denotes the Frobenius-Perron operator $\mathcal{H}G(X) \equiv \int dY \delta[X - T(Y)] G(Y)$ [11]. Let us introduce

$$E^\alpha(X) \equiv \begin{cases} 1 & \text{if } X \in R^\alpha \\ 0 & \text{otherwise} \end{cases} \tag{20}$$

and

$$E_j(X) \equiv \begin{cases} 1 & \text{if } X \in R_j \\ 0 & \text{otherwise} \end{cases} \tag{21}$$

($\alpha = 0,1, j = 0,1,2, \ldots$), then, in the present models, the linear space spanned by $\{E^\alpha(X) E_j(X)\}$ is mapped to the linear space spanned by $\{E_j(X)\}$ under the operation of the Frobenius-Perron operator $\mathcal{H}$ and $\rho(X)$, which is a fixed point of $\mathcal{H}$, can be found in the linear space spanned by $\{E_j(X)\}$. Moreover, if we are considering piecewise constant $u(X)$ in each $R^\alpha \cap R_j$ such that $u(X) = \Sigma_{\alpha,j} u_j^\alpha E^\alpha(X) E_j(X)$, which is the case in Eqs. (16) and (15), then the operation of $\mathcal{H} e^{qu(X)}$ in the linear space spanned by $\{E_j(X)\}$ is expressed with an infinite-dimensional matrix as follows:

$$\mathcal{H} e^{qu(X)} E_j(X) = \mathcal{H} e^{qu(X)} (E^0(X) + E^1(X)) E_j(X) \tag{22}$$

$$= \mathcal{H} (e^{qu_j^0} E^0(X) + e^{qu_j^1} E^1(X)) E_j(X) \tag{23}$$

$$= \sum_{i=0}^{\infty} (P_{ij}^0 e^{qu_j^0} + P_{ij}^1 e^{qu_j^1}) e_i(X) \int dY E_j(Y), \tag{24}$$

with $e_i(X) \equiv E_i(X) / \int dY E_i(Y)$ and

$$P_{ij}^0 \equiv a(\delta_{i,0} \delta_{j,0} + \delta_{i+1,j}), \tag{25}$$

$$P_{ij}^1 \equiv a' \delta_{i-1,j}, \tag{26}$$

for the model I and

$$P_{ij}^0 \equiv b'^{-1} b^i \delta_{j,0} + a \delta_{i+1,j}, \tag{27}$$

$$P_{ij}^1 \equiv a' \delta_{i-1,j} (1 - \delta_{j,0}), \tag{28}$$

for the model II, where $a' \equiv 1 - a$ and $b' \equiv 1 - b$. Thus, by introducing a matrix $[P_q]_{ij} \equiv P_{ij}^0 e^{qu_j^0} + P_{ij}^1 e^{qu_j^1}$, we obtain

$$M_n(q) = \int dX \sum_{i,j=0}^{\infty} [P_q{}^n]_{ij} p_j e_i(X) = \sum_{i,j=0}^{\infty} [P_q{}^n]_{ij} p_j, \tag{29}$$

where $p_j \equiv \int dX \rho(X) E_j(X)$. Note that, at $q = 0$, $[P_q]_{ij}$ is identified as the transition probability from the state j to the state i of an infinite Markov chain and p_i, which satisfies $p_i = \Sigma_{j=0}^\infty [P_0]_{ij} p_j$ and $\Sigma_{i=0}^\infty p_i = 1$, is obtained as

$$p_i = (a - a') a^{-1} (a'/a)^i \tag{30}$$

for the model I and

$$p_i = \begin{cases} (a - a') b' / (1 - 2a'b') & \text{if } i = 0 \\ p_0 b (a' - ab)^{-1} \{ (a'/a)^i - b^i \} & \text{if } i \geqslant 1 \end{cases} \tag{31}$$

for the model II. Note also that, for $j > 0$, in both models, $[P_0]_{ij} = a \delta_{i+1,j} + a' \delta_{i-1,j}$, which represents random walks as shown in Fig. 1 and $[P_q]_{ij} = a e^{qu_+} \delta_{i+1,j} + a' e^{qu_-} \delta_{i-1,j}$ with $u(X)$ of Eqs. (16) and (15).

By evaluating Eq. (29) for large n, we obtain $\phi(q)$ as $M_n(q) \sim e^{n\phi(q)}$. Equation (29) is rewritten as

$$M_n(q) = \sum_{\{i_0, i_1, \ldots, i_n\}} [P_q]_{i_n i_{n-1}} [P_q]_{i_{n-1} i_{n-2}} \cdots [P_q]_{i_1 i_0} p_{i_0}, \tag{32}$$

where the summation is taken over all the possible paths $\{i_0, i_1, \ldots, i_n\}$ with length n of the Markov chain. For a fixed $m > 0$, the possible paths are divided into two groups $S_n^{(m)}$ and $\overline{S_n^{(m)}}$ according to whether all the $i_0, i_1, \ldots, i_n$ are less than m or not. The contribution from the bounded paths $S_n^{(m)}$ is

$$M_n^{(m)}(q) = \sum_{\{i_0, i_1, \ldots, i_n\} \in S_n^{(m)}} [P_q]_{i_n i_{n-1}} \times [P_q]_{i_{n-1} i_{n-2}} \cdots [P_q]_{i_1 i_0} p_{i_0} \tag{33}$$

$$= \sum_{i,j=0}^{m-1} [(P_q^{(m)})^n]_{ij} p_j \sim (\lambda_q^{(m)})^n, \tag{34}$$

where $P_q^{(m)}$ denotes the $m \times m$ matrix defined by $[P_q^{(m)}]_{ij} = [P_q]_{ij} (0 \leqslant i,j < m)$ and $\lambda_q^{(m)}$ is the largest real eigenvalue of $P_q^{(m)}$. In another way, the possible paths are divided into two groups S_n^0 and $\overline{S_n^0}$ according to whether all the $i_0, i_1, \ldots, i_n$ are greater than 0 or not. If a path is in S_n^0, then the path is equivalent to a path of random walks as mentioned above. The contribution from the random walk paths S_n^0 is denoted by

$$Z_n(q) \equiv \sum_{\{i_0, i_1, \ldots, i_n\} \in S_n^0} [P_q]_{i_n i_{n-1}} \times [P_q]_{i_{n-1} i_{n-2}} \cdots [P_q]_{i_1 i_0} p_{i_0}. \tag{35}$$

It is apparent that $S_n^0 \cap \overline{S_n^{(m)}} \neq \phi$ for any $m > 0$. Since we can take an arbitrarily large value of m, the paths that repeatedly visit the state 0 are considered to be included in $S_n^{(m)}$. Thus the paths that are not included in both $S_n^{(m)}$ and S_n^0 and which we need to take into account are the paths $\{i_0, i_1, \ldots, i_n\}$

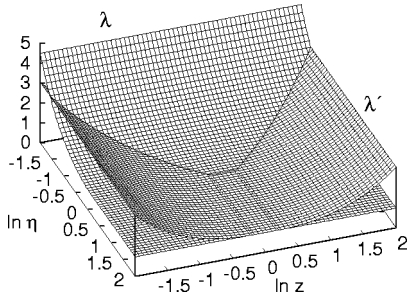

FIG. 2. Functions λ and λ′ of η and z for the model I with $a=0.6$. Both λ and λ′ reach the same minimum value $2\sqrt{aa'}$ tangentially.

such that $\{i_0,i_1,\ldots,i_l\}\in S_l^{(m)}$ and $\{i_l,i_{l+1},\ldots,i_n\}\in S_{n-l+1}^0$ with a small l compared with n, so that the exponential dependence of $M_n(q)$ on n is obtained by evaluating the sum of $M_n^{(m)}(q)$ with $m\to\infty$ and $Z_n(q)$.

As shown in Appendix C, $Z_n(q)$ is evaluated as $Z_n(q)\sim e^{nq(u_++u_-)/2}(\lambda_q')^n$. Thus we conclude that

$$e^{\phi(q)}=e^{q(u_++u_-)/2}\max\{\lambda_q,\lambda_q'\}, \tag{36}$$

where λ_q denotes $e^{-q(u_++u_-)/2}\lambda_q^{(\infty)}$.

As shown in Appendixes A and B, λ_q is obtained as a function $\lambda(\eta)$ of $\eta\equiv e^{q(u_++u_--2u_0)/2}$ for the model I and as a function $\lambda(\eta,z)$ of η and $z\equiv e^{-q(u_+-u_-)/2}$ for the model II. The minimum value of λ is $2\sqrt{aa'}$, which corresponds to the band edge of the continuous eigenvalue of $e^{-q(u_++u_-)/2}P_q$ and the first derivative of λ continuously vanishes at $\eta=\sqrt{a/a'}$ and $2\sqrt{aa'}(1-bz^{-1}\sqrt{a/a'})=b'\eta^{-1}$ for the models I and II, respectively, where the discrete real eigenvalue disappears. As shown in Appendix C, λ_q' is obtained as a function $\lambda'(z)$ of z, which has the same minimum value $2\sqrt{aa'}$ as that of λ. Note that λ and λ′ do not depend on b in the model I.

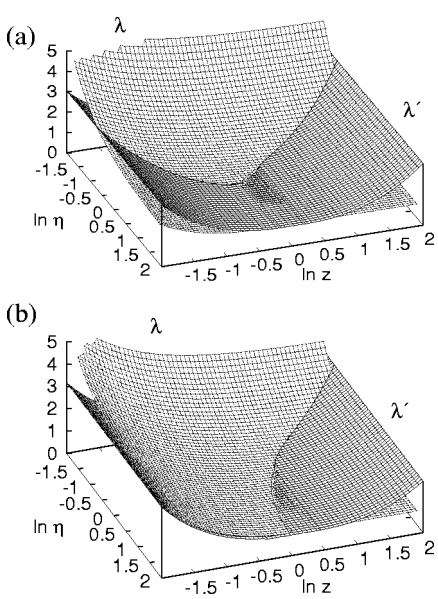

FIG. 3. Functions λ and λ′ of η and z for the model II with (a) $a=0.6$ and $b=0.4$ and (b) $a=0.7$ and $b=0.6$. Both λ and λ′ reach the same minimum value $2\sqrt{aa'}$ tangentially.

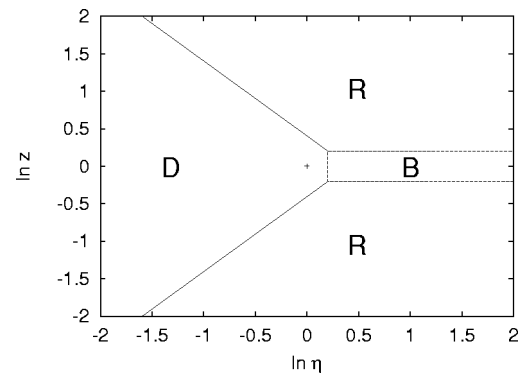

FIG. 4. Phase diagram on the η-z plane for the model I with $a=0.6$ corresponding to Fig. 2. The symbols D, R, and B denote the discrete eigenvalue, the contribution from random walks, and the band edge of continuous eigenvalue, respectively.

In Figs. 2 and 3, λ and λ′ are plotted against z and η for the models I and II. In Figs. 4 and 5, three phases D, R, and B introduced according to the relative magnitudes of λ and λ′ are shown on the η-z plane. In the phase D the discrete

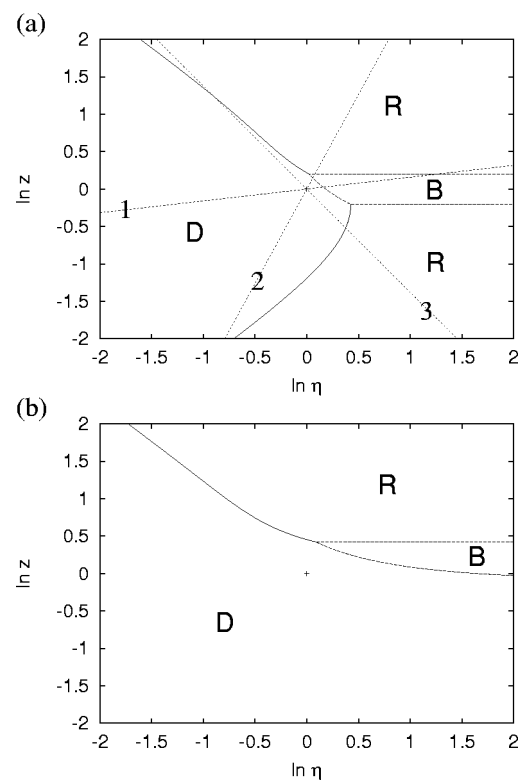

FIG. 5. Phase diagrams on the η-z plane for the model II with (a) $a=0.6$ and $b=0.4$ and (b) $a=0.7$ and $b=0.6$, corresponding to Fig. 3. The symbols D, R, and B denote the discrete eigenvalue, the contribution from random walks, and the band edge of continuous eigenvalue, respectively. If $b>a'/a$, R does not exist for $z<1$. The dotted lines 1, 2, and 3 in (a) show $\eta=e^{-q\cos\varphi}$ and $z=e^{-q\sin\varphi}$ for $-\infty<q<\infty$ with $\varphi=0.05\pi$, 0.38π, and 0.7π, respectively.

eigenvalue is dominant, i.e., $\lambda > \lambda' > 2\sqrt{a/a'}$, in the phase R the contribution from random walks is dominant, i.e., $\lambda' > \lambda > 2\sqrt{a/a'}$, and in the phase B the band edge is dominant, i.e., $\lambda' = \lambda = 2\sqrt{a/a'}$. By comparing the magnitudes of λ and λ', we obtain the boundary between the phases D and R as

$$\eta = (a/a')z^{-1} \quad (z > \sqrt{a/a'}) \tag{37}$$

and

$$\eta = (a/a')z \, (z < \sqrt{a'/a}) \tag{38}$$

for the model I and

$$\eta = \frac{a'b'z}{(a'z + az^{-1})(a'z - abz^{-1})} \, (z > \sqrt{a/a'}) \tag{39}$$

and, if $b < a'/a$,

$$\eta = \frac{a'b'}{(a' - ab)(az + a'z^{-1})} \, (z < \sqrt{a'/a}) \tag{40}$$

for the model II.

Let us fix the values of u_0 and $u_\pm$, then $[\ln \eta = q(u_+ + u_- - 2u_0)/2, \ln z = -q(u_+ - u_-)/2]$ for $-\infty < q < \infty$ is a straight line passing through the origin on the $\ln \eta$-$\ln z$ plane. By Eq. (36), a change of phases along the line on the

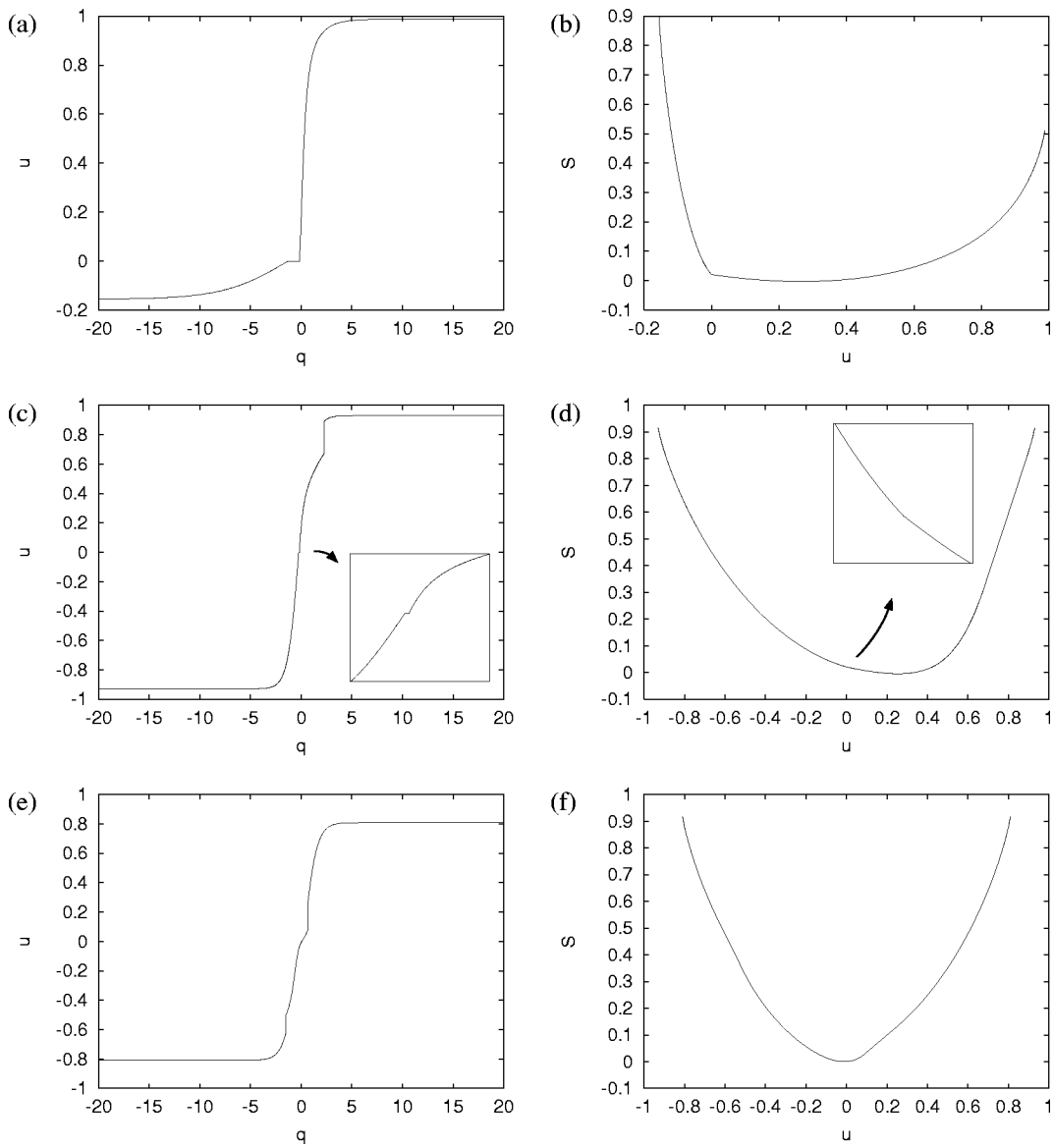

FIG. 6. The q-weighted average $u(q)$ and the fluctuation spectrum $S(u)$ for the model II with $a = 0.6$ and $b = 0.4$. Corresponding to the three dotted lines 1, 2, and 3 in Fig. 5(a), the values of $u_0 = \cos\varphi$ and $u_+ = -u_- = \sin\varphi$ are set in three ways: $\varphi = 0.05\pi$ for (a) and (b), 0.38π for (c) and (d), and 0.7π for (e) and (f). A plateau, a plateau and a jump, and two jumps are observed in (a), (c), and (e), respectively.

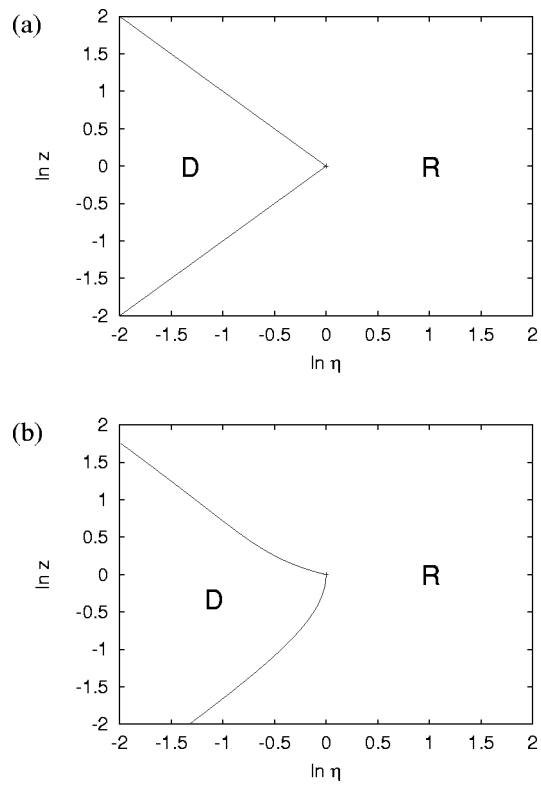

FIG. 7. Phase diagrams on the η-z plane for (a) the model I with $a=a_0$ and (b) the model II with $a=a_0$ and $b=0.6$ at the onset of on-off intermittency. In both models, at the origin the first derivatives of both λ and λ' vanish.

$\ln\eta$-$\ln z$ plane brings about a singularity in $\phi(q)$ at the corresponding value of q. At the boundary between D and R denoted by a solid line in Figs. 4 and 5, $u(q)=d\phi(q)/dq$ exhibits a jump. In the phase C, $u(q)$ is a constant since $du(q)/dq=0$ and, at its boundary denoted by a dashed line in Figs. 4 and 5, the slope $du(q)/dq$ of $u(q)$ exhibits a jump. For example, in Fig. 6, $u(q)$ and $S(u)$ are plotted for the three sets of values of u_0 and $u_\pm$ expressed as $u_0=\cos\varphi$ and $u_+=-u_-=\sin\varphi$ with $\varphi=0.05\pi$, 0.38π, and 0.7π corresponding to the three dotted lines in Fig. 5(a). Figures 6(a) and 6(b) are for the dotted line 1, where $u(q)$ has a plateau that corresponds to a salient point of $S(u)$. Figures 6(c) and 6(d) are for the dotted line 2, where $u(q)$ has a plateau and a jump that correspond to a salient point of $S(u)$ and a linear slope of $S(u)$, respectively. Figures 6(e) and 6(f) are for the dotted line 3, where $u(q)$ has two jumps that correspond to two linear slopes in $S(u)$.

In the previous paper [8], the model II with $u_0=1$ and $u_+=u_-=0$ is considered, where only the singularity at the boundary between D and B is observed or no singularity is observed according to whether $b<a'/a$ or not. Note that, as it is understood from Figs. 4 and 5, if $\ln z\equiv 0$, i.e., $u_+=u_-$, there appears only the singularity at the boundary between D and B, which implies a constant value of $u(q)$ over a semi-infinite interval of q. Here, for systems exhibiting on-off intermittency, we conjecture that if the observed quantity $u(X)$ is independent of the direction of motion from or to the invariant subspace as for the present models with

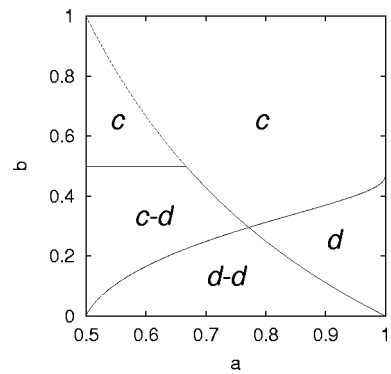

FIG. 8. Phase diagram of singularities observed in the q-weighted average of the transverse expansion rate for the model II. The symbols c and d denote a plateau and a jump in $u(q)$, respectively. The onset of on-off intermittency is at $a=a_0=1/2+0$.

$u_+=u_-$, then the only possible singularity in $u(q)$ due to on-off intermittency is a plateau over a semi-infinite interval of q. Indeed, this is also supported by the result of on-off intermittency on the multiplicative noise model [5], where $u(X)=r^2$ and r^4 are considered, with r corresponding to the distance from the invariant subspace.

Now let us consider the fluctuation of transverse expansion rate $\ln|\partial G/\partial y|$, i.e., $u_0=0$ and $u_+=-u_-=\ln b^{-1}$ for the model I and $u_0=\ln b'^{-1}$ and $u_+=-u_-=\ln b^{-1}$ for the model II. In the case of the model I, by considering the vertical line ($\ln\eta=0, \ln z=q\ln b$) with $-\infty<q<\infty$ in Fig. 4, it is confirmed that there are two jumps in $u(q)$ and corresponding two linear slopes in $S(u)$ for $a>a_0=1/2+0$. At the onset of on-off intermittency $a=a_0$, there appears no singularity since Fig. 4 converges to Fig. 7(a) in the limit of $a\to a_0$. On the other hand, in the case of the model II, a variety of behaviors as in Fig. 6 is observed depending on the values of a and b as shown in Fig. 8, where "c" denotes a plateau in $u(q)$, "d" denotes a jump in $u(q)$, and "c-d" and "d-d" denote their combinations. In the limit of $a\to a_0$, Fig. 5(b) converges to Fig. 7(b) and thus $u(q)$ exhibits a discontinuous change of its slope $du(q)/dq$ at $q=0$, as shown in Fig. 9. Corresponding to the singularity in $u(q)$ at $q=0$, the curvature of $S(u)$ shows a jump at the minimum of $S(u)$. Moreover, if $b>1/2$, a jump in $u(q)$ and a linear slope in $S(u)$ are also observed at $a=a_0$. In this way, at the onset of on-off intermittency, the degree of singularity is weakened but it becomes more probable in the sense that it appears at the minimum of $S(u)$. This singularity at the onset of on-off intermittency can be formulated by considering conditional variances of $nu_n(X)$. Let us introduce the conditional variances $\sigma^+(nu_n(X))$ and $\sigma^-(nu_n(X))$ as

$$\sigma^+(G(X))\equiv\langle\sigma(G(X)-\langle G(X)\rangle)\rangle \tag{41}$$

and $\sigma^-(G(X))\equiv\sigma^+(-G(X))$ with

$$\sigma(x)\equiv\begin{cases} x^2 & \text{if } x>0 \\ 0 & \text{otherwise.}\end{cases} \tag{42}$$

For $n\gg 1$, Eq. (11) leads to

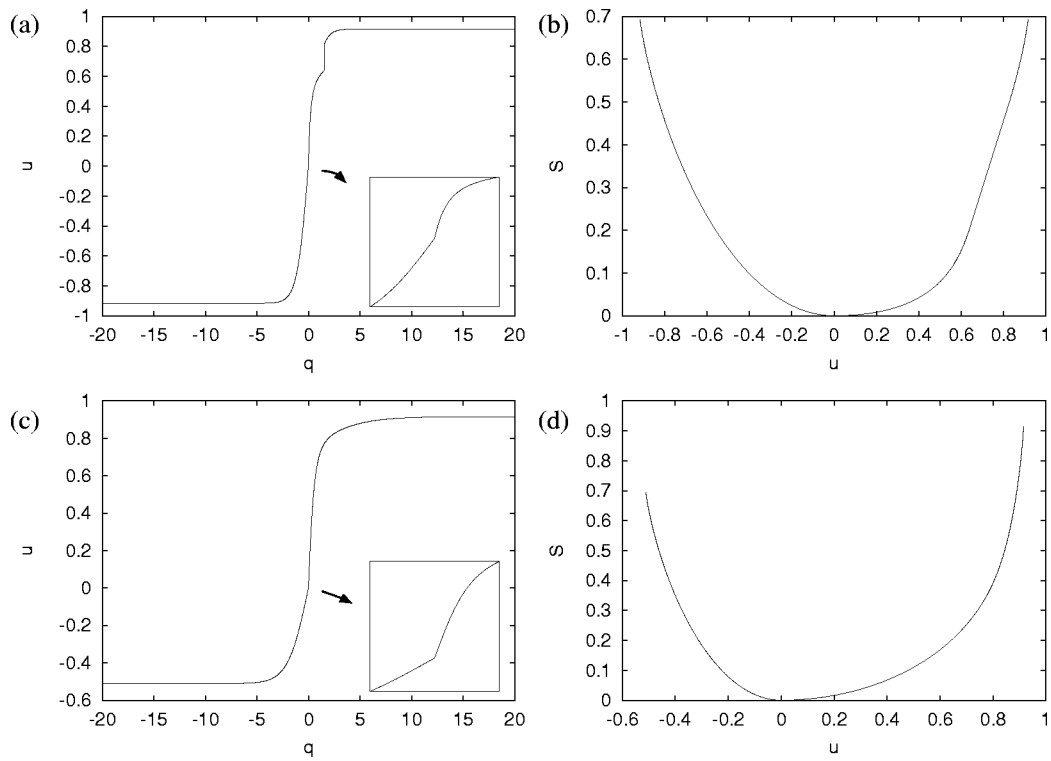

FIG. 9. The q-weighted average $u(q)$ and the fluctuation spectrum $S(u)$ of the transverse expansion rate for the model II with (a) $b=0.4$ and (b) $b=0.6$ at the onset of on-off intermittency.

$$\sigma^{+}(nu_u(X)) \sim \frac{\int_{\bar{u}}^{u_{max}} (nu)^2 e^{-nS(u)} du}{\int_{u_{min}}^{u_{max}} e^{-nS(u)} du} \tag{43}$$

$$\sim n\kappa_{+}^{-3/2}/(\kappa_{-}^{-1/2}+\kappa_{+}^{-1/2}) \tag{44}$$

and

$$\sigma^{-}(nu_u(X)) \sim n\kappa_{-}^{-3/2}/(\kappa_{-}^{-1/2}+\kappa_{+}^{-1/2}), \tag{45}$$

where, $u_{min} \equiv u(q=-\infty)$, $u_{max} \equiv u(q=\infty)$, $\bar{u} \equiv u(q=0) = \langle u(X) \rangle$, $\kappa_{\pm} \equiv d^2 S(\bar{u} \pm 0)/du^2$, and $S(u)$ is expanded around its minimum at $\bar{u}$. Thus, if $\kappa_{-} \neq \kappa_{+}$, we have different limiting values of $\sigma^{+}(nu_n(X))/n$ and $\sigma^{-}(nu_n(X))/n$.

In Fig. 10, $\sigma^{+}(nu_n(X))$ and $\sigma^{-}(nu_n(X))$ are plotted for the coupled logistic map

$$x_{n+1} = f(x_n) + \frac{1-e^{-\alpha}}{2}[f(y_n) - f(x_n)], \tag{46}$$

$$y_{n+1} = f(y_n) + \frac{1-e^{-\alpha}}{2}[f(x_n) - f(y_n)], \tag{47}$$

with $f(x) \equiv 3.8x(1-x)$, where $u(X) \equiv (x+y)/2$ is observed and the parameter value is set in two ways nearly at the onset of on-off intermittency $\alpha = 0.4321$ and out of on-off intermittency $\alpha = 0.1$. Figure 10 confirms the singularity $\kappa_{+} \neq \kappa_{-}$ at the onset of on-off intermittency. As in Figs. 4 and 5, on the $\ln \eta$-$\ln z$ plane, the origin $\ln \eta = \ln z = 0$, which corresponds to $q=0$ and the minimum of $S(u)$ is always in D except at the onset of on-off intermittency indicating that the singularities around $q=0$ and the minimum of $S(u)$ can appear only at the onset of on-off intermittency. Note that as it is understood from Fig. 7 it is possible to choose an observed quantity $u(X)$ in such a way that, at the onset of on-off intermittency, the corresponding line on the $\ln \eta$-$\ln z$ plane lies in R,

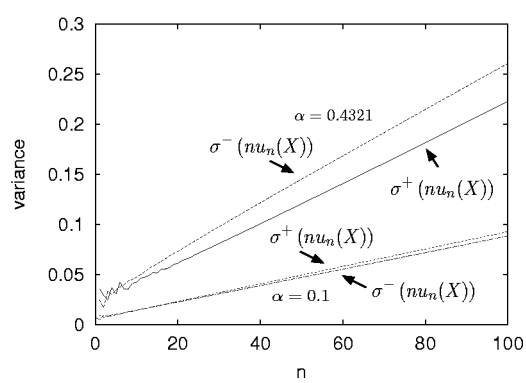

FIG. 10. Conditional variances $\sigma^{+}(nu_n(X))$ and $\sigma^{-}(nu_n(X))$ for the coupled logistic map with $\alpha = 0.432$ (upper two lines) and 0.1 (lower two lines). For $\alpha = 0.432$, the difference of the slopes of $\sigma^{+}(nu_n(X))$ and $\sigma^{-}(nu_n(X))$ confirms the discontinuity of the curvature of $S(u)$ at the minimum at the onset of on-off intermittency. The average is taken along an orbit of length 10^7.

except its origin, and no singularity in $u(q)$ appears. With such a choice of $u(X)$ near the onset of on-off intermittency, there appear two jumps in $u(q)$, which disappear at the onset of on-off intermittency.

IV. CONCLUDING REMARKS

Singularities in the fluctuation of on-off intermittency are investigated on two-dimensional piecewise linear maps. It is shown that there appear three phases of motion and by the crossover between the phases there appear singularities in $\phi(q)$ and correspondingly in $u(q)$ and $S(u)$. The q-weighted average $u(q)$ exhibits two types of singularities, a jump and a plateau. As the system approaches the onset of on-off intermittency, the width of plateau in $u(q)$ shrinks to zero, if it exists, and its position converges at $q=0$. In this way, at the onset of on-off intermittency, a jump in the slope $du(q)/dq$ of $u(q)$ at $q=0$ appears. The singularity at the onset of on-off intermittency is also confirmed for the coupled logistic map by introducing conditional variances.

In nonhyperbolic systems with homoclinic tangencies, the fluctuation of expansion rate exhibits a singularity that appears as a linear slope in $S(u)$ [12]. The singularities observed here are also related to nonhyperbolicity. In the models I and II, the tangent space at X is expressed as a direct sum $E^x(X)\oplus E^y(X)$ of the one-dimensional linear subspaces $E^x(X)$ and $E^y(X)$ along x and y directions, respectively, each of which is invariant under the tangent map, i.e., $DT(E^x(X))=E^x(T(X))$ and $DT(E^y(X)(=E^y(T(X))$. The stability in $E^y(X)$ alternates between stable and unstable depending on X within the attractor while it is always unstable in $E^x(X)$, i.e., the system posseses nonhyperbolicity called unstable dimension variability [18]. In contrast with unstable dimension variability, homoclinic tangencies are points where the unstable and stable tangent spaces degenerate such that their direct sum does not coincide with the full tangent space. In the present systems, unstable dimension variability is due to the fact that there are infinitely many paths each of which has infinite length and negative transverse Lyapunov exponent as well as infinitely many paths with positive Lyapunov exponents. Indeed, if the Markov chain shown in Fig. 1 is truncated into a finite Markov chain, then all the paths with infinite length have only positive transverse Lyapunov exponents and, moreover, only the discrete eigenvalues of P_q are possible, which implies that no singularity appears in $\phi(q)$. In this sense, the singularities observed here are considered to be due to nonhyperbolicity of on-off intermittency.

We conjecture that, for systems exhibiting on-off intermittency, the fluctuation has singularities due to nonhyperbolicity of unstable dimension variability. Finally, it should be noted that long-term numerical calculations on systems exhibiting on-off intermittency may require much care due to unstable dimension variability, which implies a breakdown of shadowing [19]. Both numerical and theoretical investigations on general systems are the subjects of future works.

ACKNOWLEDGMENTS

We wish to thank Professor H. Fujisaka, Professor S. Miyazaki, and Professor H. Hata for valuable discussions.

APPENDIX A: DISCRETE EIGENVALUES

In this appendix, the largest discrete eigenvalue of $e^{-q(u_+ + u_-)/2}P_q$ is considered.

For the model I, the truncated $m\times m$ matrix $P_q^{(m)}$ reads

$$P_q^{(m)}=\begin{pmatrix} ae^{qu_0} & ae^{qu_+} & & & & \\ a'e^{qu_-} & 0 & ae^{qu_+} & & 0 & \\ & a'e^{qu_-} & 0 & \ddots & & \\ & & a'e^{qu_-} & \ddots & ae^{qu_+} & \\ & 0 & & \ddots & 0 & ae^{qu_+} \\ & & & & a'e^{qu_-} & 0 \end{pmatrix} \tag{A1}$$

$$=e^{q(u_+ + u_-)/2}\begin{pmatrix} a\eta^{-1} & az^{-1} & & & & \\ a'z & 0 & az^{-1} & & 0 & \\ & a'z & 0 & \ddots & & \\ & & a'z & \ddots & az^{-1} & \\ & 0 & & \ddots & 0 & az^{-1} \\ & & & & a'z & 0 \end{pmatrix}, \tag{A2}$$

where $z \equiv e^{-q(u_+ - u_-)/2}$ and $\eta \equiv e^{q(u_+ + u_- - 2u_0)/2}$. Let us find λ and v satisfying ${}^t v P_q^{(m)} = e^{q(u_+ + u_-)/2} \lambda\, {}^t v$, i.e.,

$$\lambda v_1 = a\eta^{-1} v_1 + a' z v_2, \tag{A3}$$

$$\lambda v_i = a z^{-1} v_{i-1} + a' z v_{i+1}, \quad i = 2,3,\ldots,m-1, \tag{A4}$$

$$\lambda v_m = a z^{-1} v_{m-1}. \tag{A5}$$

With

$$\mu_\pm \equiv \frac{\lambda \pm \sqrt{\lambda^2 - 4aa'}}{2a'} \tag{A6}$$

and constants c_+ and c_-, Eq. (A4) can be expressed as

$$v_i = (c_+ \mu_+^{i-1} + c_- \mu_-^{i-1}) z^{-i}. \tag{A7}$$

With Eq. (A7), Eqs. (A3) and (A5) become

$$c_+(a\eta^{-1} + a'\mu_+ - \lambda) + c_-(a\eta^{-1} + a'\mu_- - \lambda) = 0 \tag{A8}$$

and

$$c_+(a - \lambda\mu_+) + c_-(\mu_-/\mu_+)^{m-2}(a - \lambda\mu_-) = 0, \tag{A9}$$

respectively. Thus,

$$c_-(\mu_-/\mu_+)^{m-2}(a - \lambda\mu_-)(a\eta^{-1} + a'\mu_+ - \lambda) = c_-(a - \lambda\mu_+)(a\eta^{-1} + a'\mu_- - \lambda). \tag{A10}$$

If $\lambda > 2\sqrt{aa'}$, then $\mu_-/\mu_+ < 1$ and with the limit of $m \to \infty$, Eq. (A10) leads to

$$\lambda = a\eta^{-1} + a'\mu_-, \tag{A11}$$

where the nonphysical solution $a - \lambda\mu_+ = 0$, which means $c_- = 0$, is abandoned. Equation (A6) is equivalent to

$$\lambda = a\mu_-^{-1} + a'\mu_-, \quad \mu_- < \sqrt{a/a'} \tag{A12}$$

and, together with Eq. (A11), this gives

$$\mu_- = \eta, \tag{A13}$$

if $\eta < \sqrt{a/a'}$. Thus, if $\eta < \sqrt{a/a'}$,

$$\lambda = a\eta^{-1} + a'\eta \tag{A14}$$

is the largest real eigenvalue of $e^{-q(u_+ + u_-)/2} P_q$ for the model I. If $\eta < \sqrt{a/a'}$ is not satisfied, there is no eigenvalue of $e^{-q(u_+ + u_-)/2} P_q$ greater than $2\sqrt{aa'}$.

For the model II, the truncated $m \times m$ matrix $P_q^{(m)}$ reads

$$P_q^{(m)} = \begin{pmatrix} b' e^{qu_0} & a e^{qu_+} & & & & \\ b' b e^{qu_0} & 0 & a e^{qu_+} & & 0 & \\ b' b^2 e^{qu_0} & a' e^{qu_-} & 0 & \ddots & & \\ b' b^3 e^{qu_0} & & a' e^{qu_-} & \ddots & a e^{qu_+} & \\ \vdots & 0 & & \ddots & 0 & a e^{qu_+} \\ b' b^{m-1} e^{qu_0} & & & & a' e^{qu_-} & 0 \end{pmatrix} \tag{A15}$$

$$= e^{q(u_+ + u_-)/2} \begin{pmatrix} b'\eta^{-1} & a z^{-1} & & & & \\ b' b \eta^{-1} & a z^{-1} & & 0 & & \\ b' b^2 \eta^{-1} & a' z & 0 & \ddots & & \\ b' b^3 \eta^{-1} & & a' z & \ddots & a z^{-1} & \\ \vdots & 0 & & \ddots & 0 & a z^{-1} \\ b' b^{m-1} \eta^{-1} & & & & a' z & 0 \end{pmatrix}. \tag{A16}$$

In a similar way as for the model I, let us find λ and v satisfying ${}^t v P_q^{(m)} = e^{q(u_+ + u_-)/2} \lambda\, {}^t v$, then Eq. (A3) is substituted by

$$\lambda v_1 = b' \eta^{-1} \sum_{i=1}^{m} b^{i-1} v_i \tag{A17}$$

and Eq. (A8) is substituted by

$$c_+\left(b'\eta^{-1} \frac{1 - (\mu_+ b z^{-1})^m}{1 - \mu_+ b z^{-1}} - \lambda \right) + c_-\left(b'\eta^{-1} \frac{1 - (\mu_- b z^{-1})^m}{1 - \mu_- b z^{-1}} - \lambda \right) = 0. \tag{A18}$$

Thus, we obtain

$$c_-(\mu_-/\mu_+)^{m-2}(a-\lambda\mu_-)\left(b'\eta^{-1}\frac{1-(\mu_+bz^{-1})^m}{1-\mu_+bz^{-1}}-\lambda\right)$$
$$=c_-(a-\lambda\mu_+)\left(b'\eta^{-1}\frac{1-(\mu_-bz^{-1})^m}{1-\mu_-bz^{-1}}-\lambda\right). \quad \text{(A19)}$$

If μ_- is real and $\mu_-bz^{-1}<1$, then, with the limit of $m\to\infty$, Eq. (A19) leads to

$$\lambda=b'\eta^{-1}/(1-\mu_-bz^{-1}), \quad \text{(A20)}$$

where the nonphysical solution $a-\lambda\mu_+=0$, which means $c_-=0$, is abandoned. Equation (A20) together with Eq. (A12) determine the largest real eigenvalue of $e^{-q(u_++u_-)/2}P_q$ for each q, which exists if

$$2\sqrt{aa'}(1-bz^{-1}\sqrt{a/a'})<b'\eta^{-1}. \quad \text{(A21)}$$

If the condition (A21) is not satisfied, then there is no eigenvalue of $e^{-q(u_++u_-)/2}P_q$ greater than $2\sqrt{aa'}$.

APPENDIX B: CONTINUOUS EIGENVALUES

In this appendix, the continuous eigenvalues of $e^{-q(u_++u_-)/2}P_q$ is considered. If $-2\sqrt{aa'}<\lambda<2\sqrt{aa'}$, with a real $\theta\in[0,\pi]$, $\mu_\pm$ and λ can be expressed as $\mu_\pm=\sqrt{a/a'}e^{\pm i\theta}$ and $\lambda=2\sqrt{aa'}\cos\theta$ and, without loss of generality, we can set $c_\pm=e^{\pm i\psi}$ with a real ψ. Equation (A5) leads to

$$\text{Re}\ [e^{i\psi}e^{im\theta}]=0 \quad \text{(B1)}$$

and it is satisfied with

$$\psi+m\theta=\frac{\pi}{2}(\text{mod}\ \ \pi). \quad \text{(B2)}$$

Note that if $\theta=0$, then $\mu_+=\mu_-$, $\psi=\pi/2(\text{mod}\ \ \pi)$ by Eq. (B2) with $\varphi(0)=\pi$, and $c_++c_-=0$, which means $v_m=0$, thus $\theta=0$ is not allowed. In the same reason, $\theta=\pi$ is also not allowed. Equations (A3) and (A17) are also converted to the form of Re $[e^{i\psi}g(\theta)]=0$, where

$$g(\theta)=\sqrt{a}\eta^{-1}-\sqrt{a'}e^{-i\theta} \quad \text{(B3)}$$

for the model I and

$$g(\theta)=b'\eta^{-1}\frac{1-(bz^{-1}\sqrt{a/a'})^m e^{im\theta}}{1-bz^{-1}\sqrt{a/a'}e^{i\theta}}-2\sqrt{aa'}\cos\theta \quad \text{(B4)}$$

for the model II, and, by eliminating ψ by Eq. (B2), it leads to

$$\gamma(\theta)=m\theta(\text{mod}\ \ \pi), \quad \text{(B5)}$$

where $\gamma(\theta)\equiv\arg\{g(\theta)\}$. For the model I, $\gamma(\theta)$ is continuous and

$$0=\gamma(0)=\gamma(\pi)\leqslant\gamma(\theta)<\pi/2 \ \text{ if } \ \eta\leqslant\sqrt{a/a'}$$
$$0=\gamma(\pi)\leqslant\gamma(\theta)\leqslant\gamma(0)=\pi \ \text{ otherwise.} \quad \text{(B6)}$$

Thus, for large m, there are $m-1$ or m almost equally spaced solutions of θ over the interval $(0,\pi)$. In the limit of $m\to\infty$, the solutions θ form an interval $[0,\pi]$ and we have a band $[-2\sqrt{aa'},2\sqrt{aa'}]$ of continuous eigenvalues of $e^{-q(u_++u_-)/2}P_q$. For the model II, we consider the case $bz^{-1}\sqrt{a/a'}<1$, otherwise the condition (A21) for the existence of the eigenvalue of $e^{-q(u_++u_-)/2}P_q$ greater than $2\sqrt{aa'}$ is automatically satisfied. For large m, $\gamma(\theta)$, whose dependence on m can be neglected, is continuous and bounded, since $g(\theta)$ converges to

$$\frac{b'\eta^{-1}}{1-bz^{-1}\sqrt{a/a'}e^{i\theta}}-2\sqrt{aa'}\cos\theta \quad \text{(B7)}$$

with $m\to\infty$. And $\gamma(\pi)=0$ and $\gamma(0)=\pi$ or 0 according to whether $g(0)\leqslant 0$ or not, thus, similarly as for the model I, we also have a band $[-2\sqrt{aa'},2\sqrt{aa'}]$ of continuous eigenvalues of $e^{-q(u_++u_-)/2}P_q$ for the model II.

APPENDIX C: EVALUATION OF $Z_n(q)$

Each element of S_n^0 is a path of random walks with length n, which never visit the state 0. Let us define

$$K(l,t)\equiv\begin{cases}{}_tC_{(l+t)/2} & \text{if } \ l=-t,-t+2,\ldots,t-2,t\\ 0 & \text{otherwise,}\end{cases} \quad \text{(C1)}$$

and let $i,j>0$. Then the number of the possible paths of length n from i to j is $K(i-j,n)-K(i+j,n)$ by the reflection principle [20]. Our purpose is to evaluate

$$Z_n(q)=\sum_{i=1}^{\infty}p_i\sum_{j=1}^{\infty}(a'e^{qu_-})^m(ae^{qu_+})^{n-m}$$
$$\times\{K(i-j,n)-K(i+j,n)\}, \quad \text{(C2)}$$

where $m\equiv(n+j-i)/2$ is the number of steps toward the positive direction. With $v\equiv\sqrt{a'/a}e^{-q(u_+-u_-)/2}$, Eq. (C2) reads

$$Z_n(q)=e^{nq(u_++u_-)/2}(aa')^{n/2}\sum_{i=1}^{\infty}p_i\sum_{j=1}^{\infty}v^{j-i}$$
$$\times\{K(i-j,n)-K(i+j,n)\}. \quad \text{(C3)}$$

Note that $p_i\propto(a'/a)^i$ and $(a'-ab)^{-1}\{(a'/a)^i-b^i\}$ for the models I and II, respectively, and let us evaluate

$$G(v,w,n)\equiv\sum_{i=1}^{\infty}\sum_{j=1}^{\infty} w^i v^{j-i}\{K(i-j,n)-K(i+j,n)\} \tag{C4}$$

$$\begin{aligned}=&\sum_{i=1}^{n} w^i \sum_{j=1-i}^{t} v^l K(j,n)\\ &+\sum_{i=n+1}^{\infty} w^i \sum_{j=-n}^{n} v^j K(j,n)\\ &-\sum_{i=1}^{n-1} (w/v^2)^i \sum_{j=i+1}^{n} v^j K(j,n),\end{aligned} \tag{C5}$$

with $0<w<1$. The second term of Eq. (C5) is

$$w^{n+1}(1-w)^{-1}\sum_{m=0}^{n} v^{2m-n}{}_nC_m=w^{n+1}(1-w)^{-1}(v^{-1}+v)^n. \tag{C6}$$

By using Stirling's formula, the first term of Eq. (C5) is approximated by

$$\begin{aligned}&n^{-1/2}\int_0^1 dr_0\int_{-r_0}^{1} dr w^{nr_0}v^{nr}\\ &\times\exp\left\{-n\left(\frac{1+r}{2}\ln\frac{1+r}{2}+\frac{1-r}{2}\ln\frac{1-r}{2}\right)\right\}.\end{aligned} \tag{C7}$$

Since $w<1$, the maximum of the integrand is achieved at a point on $\{(r_0,r)|r_0=0,0\leqslant r\leqslant 1\}\cup\{(r_0,r)|0\leqslant r_0=-r\leqslant 1\}$ and thus Eq. (C7) is evaluated as

$$\begin{aligned}&(v^{-1}+v)^n \quad \text{if} \quad v>1,\\ &2^n \quad \text{if} \quad w\leqslant v\leqslant 1,\\ &(v^{-1}w+vw^{-1})^n \quad \text{if} \quad v<w.\end{aligned} \tag{C8}$$

Similarly, the third term of Eq. (C5) is evaluated and its contribution can be neglected. Since $w<1$, Eqs. (C6) and (C8) lead to

$$G(v,w,n)\sim\begin{cases}(v^{-1}+v)^n & \text{if } v>1\\ 2^n & \text{if } w\leqslant v\leqslant 1\\ (v^{-1}w+vw^{-1})^n & \text{if } v<w.\end{cases} \tag{C9}$$

Thus, Eqs. (C3) and (C9) lead to

$$\begin{aligned}&\lim_{n\to\infty} Z_n(q)^{1/n}\\ &=\begin{cases}ae^{qu_+}+a'e^{qu_-} & \text{if } ae^{qu_+}<a'e^{qu_-}\\ awe^{qu_+}+a'w^{-1}e^{qu_-} & \text{if } awe^{qu_+}>a'w^{-1}e^{qu_-}\\ 2\sqrt{aa'}e^{q(u_++u_-)/2} & \text{otherwise,}\end{cases}\end{aligned} \tag{C10}$$

where $w=a'/a$ and $\max\{a'/a,b\}$ for the models I and II, respectively. With $z=e^{-q(u_+-u_-)/2}$ and

$$\lambda_q'\equiv\begin{cases}az^{-1}+a'z & \text{if } az^{-1}<a'z\\ awz^{-1}+a'w^{-1}z & \text{if } awz^{-1}>a'w^{-1}z\\ 2\sqrt{aa'} & \text{otherwise,}\end{cases} \tag{C11}$$

Eq. (C10) is expressed as $Z_n(q)\sim e^{nq(u_++u_-)/2}(\lambda_q')^n$. Note that the minimum value $2\sqrt{aa'}$ of λ_q' coincides with the band edge of the continuous eigenvalue of $e^{-q(u_++u_-)/2}P_q$ and the first derivative of λ_q' continuously vanishes at $z=w\sqrt{a/a'}$ and $\sqrt{a/a'}$ and equals to 0 between them.

[1] H. Fujisaka and T. Yamada, Prog. Theor. Phys. **74**, 918 (1985); **75**, 1087 (1986).

[2] N. Platt, E.A. Spiegel, and C. Tresser, Phys. Rev. Lett. **70**, 279 (1993).

[3] J.C. Alexander, J.A. Yorke, Z. You, and I. Kan, Int. J. Bifurcation Chaos Appl. Sci. Eng. **2**, 795 (1992).

[4] See, e.g., T. Yamada and H. Fujisaka, Prog. Theor. Phys. **76,** 582 (1986); H. Fujisaka and T. Yamada, *ibid.* **77**, 1045 (1987); T. Yamada, K. Fukushima, and T. Yazaki, Prog. Theor. Phys. Suppl. **99**, 120 (1989); J.F. Heagy, N. Platt, and S.M. Hammel, Phys. Rev. E **49**, 1140 (1994); N. Platt, S.M. Hammel, and J.F. Heagy, Phys. Rev. Lett. **72**, 3498 (1994); Y.-C. Lai and C. Grebogi, Phys. Rev. E **52**, R3313 (1995); S.C. Venkataramani, T.M. Antonsen, Jr., E. Ott, and J.C. Sommerer, Phys. Lett. A **207**, 173 (1995); Physica D **96**, 66 (1996); A. Čenys, A. Namajūnas, A. Tamaševičius, and T. Schneider, Phys. Lett. A **213**, 259 (1996); Y.-C. Lai, Phys. Rev. E **53**, R4267 (1996); **54**, 321 (1996); H. Fujisaka, S. Matsushita, and T. Yamada, J. Phys. A **30**, 5697 (1997); S. Miyazaki and H. Hata, Phys. Rev. E **58**, 7172 (1998); T. Harada, H. Hata, and H. Fujisaka, J. Phys. A **32**, 1557 (1999); S. Miyazaki, J. Phys. Soc. Jpn. **69**, 2719 (2000); H. Fujisaka, H. Suetani, and T. Watanabe, Prog. Theor. Phys. Suppl. **139**, 70 (2000).

[5] T. Yamada and H. Fujisaka, Prog. Theor. Phys. **84**, 824 (1990); H. Fujisaka and T. Yamada, *ibid.* **90**, 529 (1993).

[6] E. Ott and J.C. Sommerer, Phys. Lett. A **188**, 39 (1994).

[7] H. Hata and S. Miyazaki, Phys. Rev. E **55**, 5311 (1997).

[8] H. Suetani and T. Horita, Phys. Rev. E **60**, 422 (1999).

[9] H. Fujisaka, K. Ouchi, H. Hata, B. Masaoka, and S. Miyazaki, Physica D **114**, 237 (1998); T. John, R. Stannarius, and U. Behn, Phys. Rev. Lett. **83**, 749 (1999); H. Fujisaka, K. Ouchi, and H. Ohara, Phys. Rev. E **64**, 036201 (2001).

[10] See, e.g., H. Mori and Y. Kuramoto, *Dissipative Structures and Chaos* (Springer-Verlag, Berlin, 1998); R. Badii and R. Politi, *Complexity–Hierarchical Structures and Scaling in Physics* (Cambridge University Press, Cambridge, England, 1997); C. Beck and F. Schlögl, *Thermodynamics of Chaotic Systems. An Introduction* (Cambridge University Press, Cambridge, England, 1993).

[11] H. Fujisaka and M. Inoue, Prog. Theor. Phys. **77**, 1334 (1987); Phys. Rev. A **39**, 1376 (1989).

[12] H. Hata, T. Horita, H. Mori, T. Morita, and K. Tomita, Prog. Theor. Phys. **80**, 809 (1988); P. Grassberger, R. Baddi, and A. Politi, J. Stat. Phys. **51**, 135 (1988); J. Peinke, J. Parisi, O. E. Rössler, and R. Stoop, *Encounter with Chaos* (Springer-Verlag, Berlin, 1992), Sec. 4.3; T. Horita and H. Mori, Prog. Theor. Phys. **91**, 677 (1994).
[13] H. Suetani and T. Horita, Chaos **11**, 795 (2001).
[14] G. Radons, Phys. Rep. **290**, 67 (1997); **75**, 4719 (1995).
[15] J. Milnor, Commun. Math. Phys. **99**, 177 (1985).
[16] See, e.g., C. Beck and F. Schlögl, p. 153 in Ref. [10].
[17] For a general description of large deviation theory, see, e.g., J. C. Bucklew, *Large Deviation Techniques in Decision, Simulation and Estimation* (Wiley, New York, 1990).
[18] R. Abraham and S. Smale, Proc. Symp. Pure Math. **14**, 5 (1970); E.J. Kostelich, I. Kan, C. Grebigi, E. Ott, and J.A. Yorke, Physica D **109**, 81 (1997).
[19] S. Dawson, C. Grebogi, T. Sauer, and J.A. Yorke, Phys. Rev. Lett. **73**, 1927 (1994); Y.-C. Lai and C. Grebogi, *ibid.* **82**, 4803 (1999); E. Barreto and P. So, *ibid.* **85**, 2490 (2000).
[20] See, e.g., W. Feller, *An Introduction to Probability Theory and Its Applications* (Wiley, New York, 1968), p. 72.